J Eng Math (2007) 57:41–55
DOI 10.1007/s10665-006-9070-1

ORIGINAL PAPER

Computing elliptic membrane high frequencies by Mathieu and Galerkin methods

Howard B. Wilson · Robert W. Scharstein

Received: 15 March 2005 / Accepted: 10 July 2006 / Published online: 21 September 2006

Abstract Resonant modes of an elliptic membrane are computed for a wide range of frequencies using a Galerkin formulation. Results are confirmed using Mathieu functions and finite-element methods. Algorithms and their implementations are described to handle Dirichlet or Neumann boundary conditions and draw animations or contour plots of the modal surfaces. The methods agree to four or more digit accuracy for the first one hundred modes. The effects of high function order and high frequency parameter upon the convergence of the modified Mathieu function series are discussed and quantified. The Galerkin method is conceptually simple and requires only an eigenvalue solver without the need of special functions.

Keywords Special functions · Natural frequencies · Waveguide modes · Eigenvalues

1 Introduction

This study compares three different methods to compute natural frequencies and mode shapes of an elliptic membrane having either a Dirichlet- or a Neumann-type boundary condition. The classical method using elliptic coordinates and transcendental Mathieu functions is discussed in Sect. 2. Numerical implementation of the classical method involves approximations pertaining to the characteristic values and the truncated infinite series. The Galerkin formulation of Sect. 3 uses elliptic coordinates and trigonometric series which exactly satisfy the boundary conditions and approximately satisfy the differential equations. Comparable finite-element results using cubic triangular elements are also presented.

Although Mathieu functions are not as common as some of the more easily computed eigenfunctions that result from separating the wave equation in curvilinear coordinates, they are useful in various applications. A secondary contribution of the present paper is a library of MATLAB routines to compute the angular (periodic) and the radial (modified) Mathieu functions for a wide range of orders and real parameters. These routines yield high resonant frequencies of an elliptic membrane and compare well

H. B. Wilson
University of Alabama, Aerospace Engineering Department, 205 Hardaway Hall, Tuscaloosa, AL 35487-0280, USA

R. W. Scharstein (✉)
University of Alabama, Electrical Engineering Department, 317 Houser Hall, Tuscaloosa, AL 35487-0286, USA
e-mail: rscharst@bama.ua.edu

with the Galerkin method. Both Dirichlet (soft) and Neumann (hard) boundary conditions are addressed. Although low-frequency results from a wide range of numerical and approximate techniques are scattered among various application-oriented papers, high frequency data have not been available.

The fundamental reference works on Mathieu functions are the books by McLachlan [1], Meixner and Schäfke [2] and the chapter by Blanch in Abramowitz and Stegun [3, Chapter 20]. Useful Fortran-based routines are discussed by Zhang and Jin [4, Chapter 14]. The tutorial [5] by Gutiérrez-Vega et al. summarizes several applications of Mathieu's differential equation, and interesting as well as accurate curves are presented. The insightful paper [6] by Chen et al. relates modern numerical evaluation to some of the asymptotic predictions by Keller and Rubinow [7]. In particular, Chen et al. draw attention to three distinct classes of high-frequency modes that can exist on the elliptic membrane; whispering gallery, bouncing ball, and focus modes. The absence of explicit formulae, integral or otherwise, makes asymptotic analysis more difficult for Mathieu functions than for Bessel functions, for example. In addition to the classic high frequency results of Keller and Rubinow [7], which are based on the WKB extension of geometrical optics, the approximate treatments of [8–10] are significant. Starting from the Rayleigh–Ritz variational formulation, Akulenko and Nesterov [8] compute the lower resonant frequencies for ellipses ranging from nearly circular (low eccentricity) to extremely flattened (high eccentricity). Troesch and Troesch [9] use Newton's method to find the roots from the Fourier-series expressions for the appropriate modified Mathieu functions. They list asymptotic approximations for the larger roots. Most notable are Troesch and Troesch's physical observations of dimensionless parameters that are remarkably stationary over a range of modes and ellipticities. Ancey et al. [10] obtain accurate values for the whispering gallery class of frequencies, in the case of the Dirichlet boundary condition, via the Langer–Olver asymptotic method applied directly to Mathieu's differential equation. A library of C++ routines developed by Alhargan [11–13] is available from the ACM Digital Library to evaluate both angular and radial Mathieu functions for orders up to 200 and q-values up to 160,000.

Hunter and Kuriyan [14] perform a series expansion for the simplified form of the modified Mathieu functions as the argument approaches infinity. The numerical work of Canosa [15] is concerned with computing the eigenvalues for the separation constant (α in (7) and (8), below). This was regarded by all of the classical authors as the key analytic step to evaluate Mathieu functions, and indeed is still an important aspect if asymptotic insight, rather than numerical data, is the goal. This is exemplified in the asymptotic analysis of Frenkel and Portugal [16]. In contrast, beginning with Stamnes and Spjelkavik [17], many recent numericists [5, 6, 11–13, 17–19, 20] exploit the computer's ability to rapidly solve the underlying eigenvalue problem for large tri-diagonal matrices. Some appreciation for the interest of microwave engineers in having tables of resonant frequencies (cutoff wavenumbers) of elliptical waveguides is clear upon examining [18] and [19]. A recent example appears with Schrödinger's equation and a periodic potential in the asymptotic evaluation of Mathieu-related functions by Aunola [21].

2 Elliptic coordinates and Mathieu functions

The historical summary of McLachlan [1, pp. 1–9] indicates that the theory of Mathieu functions is quite old. Nevertheless, provision of both the angular and the radial functions as standard library components is still uncommon. A brief outline of the origin of Mathieu's Sturm–Liouville differential equation in the context of the elliptical membrane problem is useful to define the parameters and clarify the notation.

Separating variables in the Helmholtz equation in elliptic coordinates (ξ, η) gives two ordinary differential equations involving a separation constant α and a frequency-dependent parameter q. The two-parameter dependence makes computing Mathieu functions more involved than, for example, Bessel functions. In fact, Arfken and Weber [22, p. 872] recently observed that "It is this parameter dependence that complicates the analysis of Mathieu functions and makes them among the most difficult functions used in physics."

When periodic solutions of the angular Mathieu equation are sought as Fourier series, an eigenvalue problem results which, for fixed q, gives an infinite number of real values and accompanying eigenvectors which can be normalized to yield coefficients in the Fourier series. The periodic angular functions $\mathrm{ce}_m(\eta, q)$ and $\mathrm{se}_m(\eta, q)$ must be recomputed for each choice of parameter q. As for the radial Mathieu equation, McLachlan [1, p. 26] defines its solutions as $\mathrm{Ce}_n(\xi, q) = \mathrm{ce}_n(\mathrm{i}\xi, q)$ and $\mathrm{Se}_n(\xi, q) = \mathrm{se}_n(\mathrm{i}\xi, q)$. The radial functions are most efficiently evaluated using infinite series involving Bessel functions and the series coefficients from the angular functions. Finally, exact values of the natural frequencies can then be obtained from q-values which make $\mathrm{Ce}_n(\xi_0, q) = 0$ and $\mathrm{Se}_n(\xi_0, q) = 0$.

Consider the modal vibration problem for an elliptic membrane having semi-major diameter a and semi-minor diameter b as shown in Fig. 1. The governing Helmholtz equation is

$$\left(\nabla^2 + k^2\right) \psi(x, y) = 0, \tag{1}$$

where the wavenumber is $k = \omega/c$, in terms of the radian frequency ω and the wave speed c. Under the mechanical-vibrations interpretation, the wave function ψ represents the normal displacement of a thin elastic membrane stretched over the elliptic boundary curve. The analysis leads to an eigenvalue problem involving an infinite set of eigenvalues k_n and eigenfunctions $\psi_n(x, y)$. Some common applications for this boundary-value problem model the propagation of electromagnetic or acoustic waves in cylindrical pipes of elliptic cross-section. The Dirichlet boundary condition on ψ applies to the axial component of the electric-field intensity for transverse magnetic (TM or E) modes in a hollow metal pipe, as well as to the velocity potential of an acoustic mode propagating down a waveguide with acoustically *soft* walls. If ψ represents the axial component of the magnetic field intensity for transverse electric (TE or H) modes, or the acoustic velocity potential for sound waves propagating down an acoustically *hard* walled-pipe, then the Neumann boundary condition holds. Since k is a spatial frequency, we adopt the traditional language and refer to these eigenvalues as the resonant frequencies of the elliptic membrane. Acousticians and microwave engineers typically refer to these eigenvalues as the cutoff wavenumbers. Numerical results are presented in Sects. 4 and 5 in terms of the dimensionless frequency parameter ka for a fixed value of b/a.

Formulating the problem in elliptic cylinder coordinates (ξ, η) involves the coordinate change

$$x + \mathrm{i}y = h \cosh(\xi + \mathrm{i}\eta). \tag{2}$$

The semi-focal diameter of the ellipse having the boundary

$$(x/a)^2 + (y/b)^2 = 1 \tag{3}$$

is

$$h = \sqrt{a^2 - b^2} = ae, \tag{4}$$

where e is the eccentricity. The interior is the region

$$0 \le \xi \le \xi_0 = \tanh^{-1}(b/a), \quad -\pi \le \eta \le \pi. \tag{5}$$

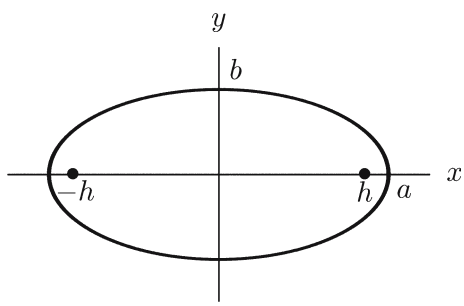

Fig. 1 Elliptic membrane

Several contours of constant ξ and η are drawn in Fig. 2. The differential equation (1) now becomes

$$\left[\frac{\partial^2}{\partial\xi^2}+\frac{\partial^2}{\partial\eta^2}+(kh)^2\left(\cosh^2\xi-\cos^2\eta\right)\right]\psi(\xi,\eta)=0, \tag{6}$$

which has product solutions of the form $\psi(\xi,\eta)=u(\xi)v(\eta)$. The separation-of-variables procedure requires satisfaction of the circumferential (or ordinary) Mathieu equation

$$v''(\eta)+(\alpha-2q\cos 2\eta)v(\eta)=0 \tag{7}$$

and the radial (or modified) Mathieu equation

$$u''(\xi)-(\alpha-2q\cosh 2\xi)u(\xi)=0. \tag{8}$$

The parameter q is related to the (spatial) frequency by

$$q=\tfrac{1}{4}(kh)^2=\tfrac{1}{4}(ka)^2[1-(b/a)^2] \tag{9}$$

and α is a separation constant which, for a fixed value of k, takes on a discrete spectrum of values providing periodic solutions for the angular Mathieu functions. Throughout this presentation, McLachlan's [1] notation is used for the Mathieu functions, as adopted by many of the subsequent standard works such as [2–4]. One minor departure is the substitution of the symbol α for McLachlan's separation constant a, because a and b are the ellipse semi-diameters.

Periodic solutions of the circumferential Mathieu equation can be found in the form

$$\mathrm{ce}_{2n+p}(\eta,q)=\sum_{m=0}^{\infty}A_{2m+p}^{2n+p}\cos(2m+p)\eta\quad(n\geq 0;\ \ p=0,1), \tag{10}$$

possessing even symmetry with respect to the x-axis, and

$$\mathrm{se}_{2n+p}(\eta,q)=\sum_{m=0}^{\infty}B_{2m+p}^{2n+p}\sin(2m+p)\eta\quad(n\geq 0;\ \ p=0,1), \tag{11}$$

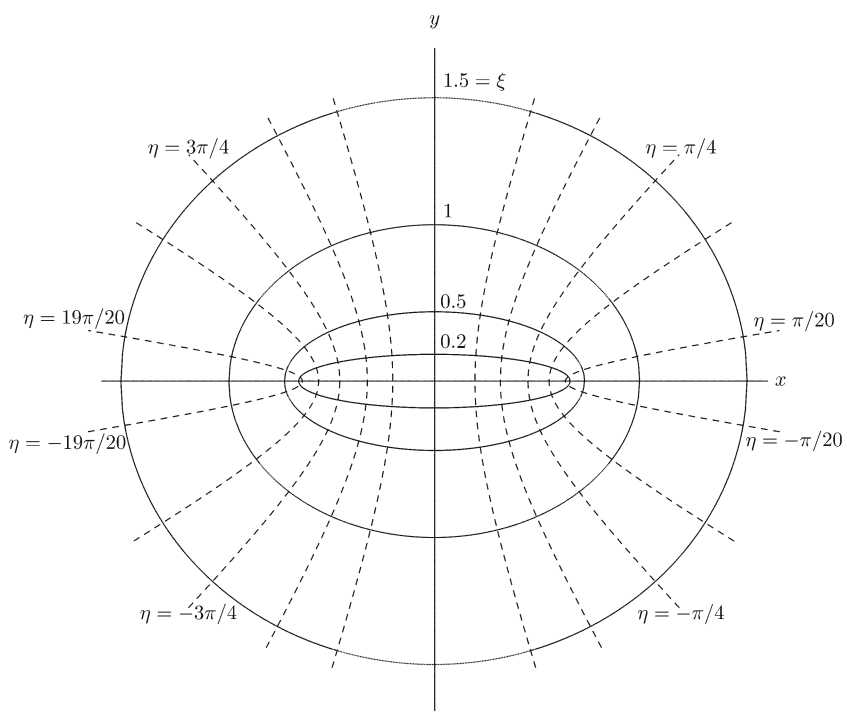

Fig. 2 Contours of constant ξ and η on the (x,y)-plane

exhibiting odd symmetry about the x-axis. So there are four periodic solution forms having series coefficients dependent upon the frequency parameter q. The resonant frequency values ka must be determined by imposing the boundary conditions.

Consider the typical procedure for determining $\mathrm{ce}_{2n}(\eta, q)$. Substituting the series (10) in the differential equation (7) leads to a homogeneous set of three-term recursion relations

$$\left[\alpha - (2m)^2\right] A_{2m}^{2n} - q\left(A_{2m-2}^{2n} + A_{2m+2}^{2n}\right) = 0 \quad (m \geq 2) \tag{12}$$

among the coefficients A_{2m}^{2n}. For a fixed q-value, this tri-diagonal matrix equation amounts to an infinite-order eigenvalue problem where α is the eigenvalue parameter, and A_{2m}^{2n} are eigenvector components. If we assume that A_{2m}^{2n} are negligibly small for m greater than or equal to some value M, then a finite-order eigenvalue problem involving the vector $[A_0^{2n}, A_2^{2n}, \ldots, A_{2M-2}^{2n}]$ results. The α-values all turn out to be real and this type of problem can be efficiently handled by a tri-diagonal eigenvalue solver. The same sort of process just described for ce_{2n} also applies for the other three periodic solutions.

Now consider solutions of the radial Mathieu equation. The modified Mathieu functions of the first kind are regular at the origin ($\xi = 0$) and are expressed as infinite series involving Bessel function products. The chosen solution forms are described by equations 20.6.7 through 20.6.10 of [3]:

$$\mathrm{Mc}_{2n}^{(1)}(\xi, q) = \sum_{m=0}^{\infty} \frac{(-1)^{m+n} A_{2m}^{2n}}{(2 - \delta_{0s}) A_{2s}^{2n}} [J_{m-s}(u_-) J_{m+s}(u_+) + J_{m+s}(u_-) J_{m-s}(u_+)], \tag{13}$$

$$\mathrm{Mc}_{2n+1}^{(1)}(\xi, q) = \sum_{m=0}^{\infty} \frac{(-1)^{m+n} A_{2m+1}^{2n+1}}{A_{2s+1}^{2n+1}} [J_{m-s}(u_-) J_{m+s+1}(u_+) + J_{m+s+1}(u_-) J_{m-s}(u_+)], \tag{14}$$

$$\mathrm{Ms}_{2n}^{(1)}(\xi, q) = \sum_{m=1}^{\infty} \frac{(-1)^{m+n} B_{2m}^{2n}}{B_{2s}^{2n}} [J_{m-s}(u_-) J_{m+s}(u_+) - J_{m+s}(u_-) J_{m-s}(u_+)], \tag{15}$$

$$\mathrm{Ms}_{2n+1}^{(1)}(\xi, q) = \sum_{m=0}^{\infty} \frac{(-1)^{m+n} B_{2m+1}^{2n+1}}{B_{2s+1}^{2n+1}} [J_{m-s}(u_-) J_{m+s+1}(u_+) - J_{m+s+1}(u_-) J_{m-s}(u_+)] \tag{16}$$

with

$$u_{\mp} = \sqrt{q} \mathrm{e}^{\mp \xi}. \tag{17}$$

The curious parameter s is chosen to improve series convergence according to the procedure described following 20.4.13 of [3]. The values of u_- and u_+ influence the convergence rates of the last four series. On the boundary, $\xi = \xi_0$ as in (5) and

$$u_{\mp} = \tfrac{1}{2} ka(1 \mp b/a). \tag{18}$$

Determining the natural frequencies entails computing a sequence of zeros (in q) of the functions $\mathrm{Mc}_n^{(1)}(\xi_0, q)$ and $\mathrm{Ms}_n^{(1)}(\xi_0, q)$ for each of a sequence of n-values. The numerical results of Sect. 4 show that the frequency values ka change more slowly between successive function orders than between successive roots for a particular order n. For example, calculation of the lowest 100 frequencies may require consideration of fairly high function orders, even though the first several roots for the lowest-order function may give high frequencies. The modal functions symmetric about the x-axis are

$$\psi(\xi, \eta) = \mathrm{Mc}_n^{(1)}(\xi, q_{n_j}) \mathrm{ce}_n(\eta, q_{n_j}), \tag{19}$$

subject to

$$\mathrm{Mc}_n^{(1)}(\xi_0, q_{n_j}) = 0, \tag{20}$$

while the anti-symmetric modal functions are

$$\psi(\xi, \eta) = \mathrm{Ms}_n^{(1)}(\xi, \hat{q}_{n_j}) \mathrm{se}_n(\eta, \hat{q}_{n_j}) \tag{21}$$

with

$$\mathrm{Ms}_n^{(1)}(\xi_0, \hat{q}_{n_j}) = 0. \tag{22}$$

3 Galerkin approximation

A different procedure employed by Wilson, Turcotte and Halpern [23, pp. 450–452] is studied here; it uses elliptic coordinates, *without* Mathieu functions, in a discretized Galerkin-type scheme with a large number of sampling points. Kantorovich and Krylov [24, p. 261] describe the Galerkin method for an approximate solution of a linear differential equation as follows. An approximate solution is constructed as a linear combination of basis functions, and the error is required to be orthogonal to each of the basis functions. The resulting system of linear equations is solved for the series coefficients. Instead of integrating to get the simultaneous equation coefficients, one evaluates the basis functions at a large set of collocation points and the discretized solution error is made orthogonal to the discretized basis vectors.

Construct series of the form

$$u(\xi) = \sum_{\ell=1}^{L} b_\ell g_\ell(\xi), \quad v(\eta) = \sum_{m=1}^{M} a_m f_m(\eta), \tag{23}$$

where

$$g_\ell(\xi) f_m(\eta) = \cos[(\ell - 1/2)\pi\xi/\xi_0]\cos[(m-1)\eta] \tag{24}$$

for even modes, and

$$g_\ell(\xi) f_m(\eta) = \sin[\ell\pi\xi/\xi_0]\sin[m\eta] \tag{25}$$

for odd modes. These forms satisfy the Dirichlet boundary conditions exactly. Choose a set of collocation points η_i ($i = 1, 2, \ldots, I$), where $I \gg M$ and substitute in the angular differential equation (7) to give

$$\sum_{m=1}^{M} a_m f_m''(\eta_i) + \alpha \sum_{m=1}^{M} a_m f_m(\eta_i) - 2q\cos(2\eta_i) \sum_{m=1}^{M} a_m f_m(\eta_i) = 0. \tag{26}$$

Let F denote the matrix with the element in row i and column m being $f_m(\eta_i)$. Multiplying (26) by the generalized inverse of F produces a matrix equation of the form

$$CA + \alpha A - qDA = 0, \tag{27}$$

where A is the column matrix $[a_m]$. A similar process with the radial equation (8) gives

$$EB - \alpha B + qGB = 0, \tag{28}$$

where $B = [b_m]$. Eliminating α from the last two equations yields

$$WE^T + CW = q(DW - WG^T) \tag{29}$$

with $W = [AB^T] = [a_i b_j]$. As shown in [23, pp. 450–452], the result (29) can be rearranged into an ordinary eigenvalue problem of order $M \times L$ in terms of the eigenvalues q and the corresponding modal coefficients. This simple method is also readily adaptable to treat the Neumann-type boundary condition by taking $g_\ell(\xi) = \cos(\ell\pi\xi/\xi_0)$ for even modes or $g_\ell(\xi) = \sin[(\ell - 1/2)\pi\xi/\xi_0]$ for odd modes of the hard ellipse.

The often-cited paper [25] by Fox, Henrici and Moler considers eigenvalues of elliptic operators and derives error bounds for modal functions which exactly satisfy the Helmholtz equation and approximately satisfy homogeneous Dirichlet boundary conditions. By applying point matching with a series involving Bessel functions, these authors compute the first 20 natural modes of an L-shaped membrane to high accuracy with inclusion of error bounds. Whereas the numerics in [25] search for zeros of a determinant, Moler [20] recently reformulated the analysis to seek minima of the smallest singular value of a matrix. The present authors tried to use this SVD-based method to compute the first 100 frequencies of an elliptic membrane, but were unable to avoid skipping over some high frequencies, even when a small search increment was used. The method worked exceptionally well for low frequencies.

Two other interesting references reporting high-accuracy frequency calculations are the work by Driscoll [26] on polygonal shaped isospectral drums and the work by Platte and Driscoll [27] which uses radial basis functions to analyze circular, L-shaped, and rhombus geometries. This reference treats both Dirichlet and Neumann boundary conditions, obtains the first 12 frequencies, and discusses how boundary-point clustering affects solutions.

4 Numerical evaluation using Mathieu functions

A group of functions is developed to evaluate the Fourier series expansions of the $\mathrm{ce}_n(\eta, q)$, $\mathrm{se}_n(\eta, q)$, and their first derivatives with respect to η. Series involving Bessel functions are also evaluated for the radial functions $\mathrm{Mc}_n^{(1)}(\xi, q)$, $\mathrm{Ms}_n^{(1)}(\xi, q)$, and their derivatives with respect to ξ. The routines make efficient use of the intrinsic matrix features of MATLAB and the Bessel functions which accept vector arguments. These functions are incorporated into a program to compute elliptic membrane frequencies and mode shapes for both Dirichlet- and Neumann-type boundary conditions. Output showing animated surface plots and contour plots is provided for modes that are either symmetric or anti-symmetric about the x-axis. The program includes a rootfinder which produces a table of frequencies obtained by varying ka, for fixed a and b, and finding zeros of $\mathrm{Mc}_n^{(1)}(\xi, q)$, $\mathrm{Ms}_n^{(1)}(\xi, q)$, $\mathrm{d}/\mathrm{d}\xi\, \mathrm{Mc}_n^{(1)}(\xi, q)$, and $\mathrm{d}/\mathrm{d}\xi\, \mathrm{Ms}_n^{(1)}(\xi, q)$ for a sequence of function orders. The frequency table is sorted in ascending order and mode shapes are presented accordingly. The program is available for download from the MathWorks software archive [28].

Figures 3–5 show example surface and contour plots obtained for Dirichlet (soft) and Neumann (hard) boundary conditions, for an ellipse having $a = 2b$. Classical series expansions described in [1, 3, 4] are used. The $E^e_{12,1}$ mode of Fig. 3 is a "focus" type, the $E^e_{0,4}$ mode of Fig. 4 is a "bouncing ball" type, and

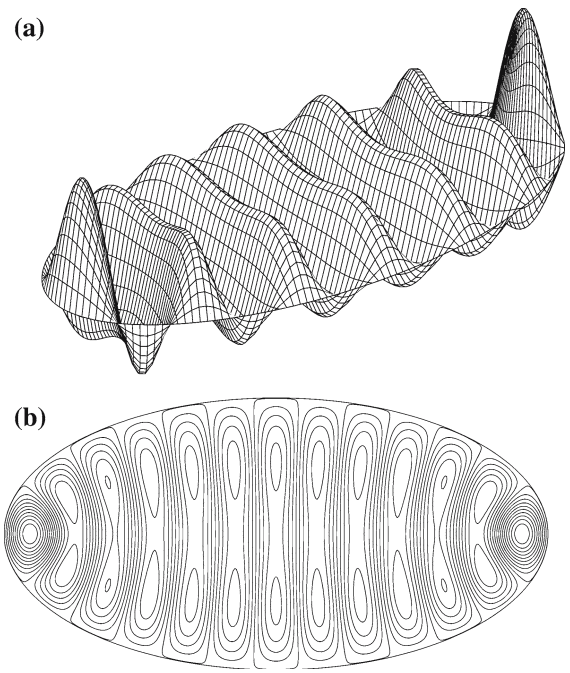

Fig. 3 Even soft mode 27 or $E^e_{12,1}$, $b/a = 1/2$, $ka = 20.85843762$. (**a**) Perspective view of ψ, (**b**) Contours of constant ψ

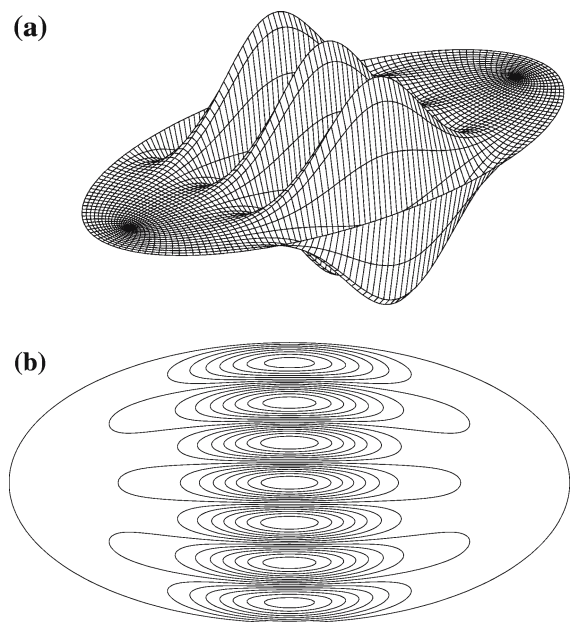

Fig. 4 Even soft mode 32 or $E^e_{0,4}$, $b/a = 1/2$, $ka = 22.52649685$. (**a**) Perspective View of ψ, (**b**) Contours of constant ψ

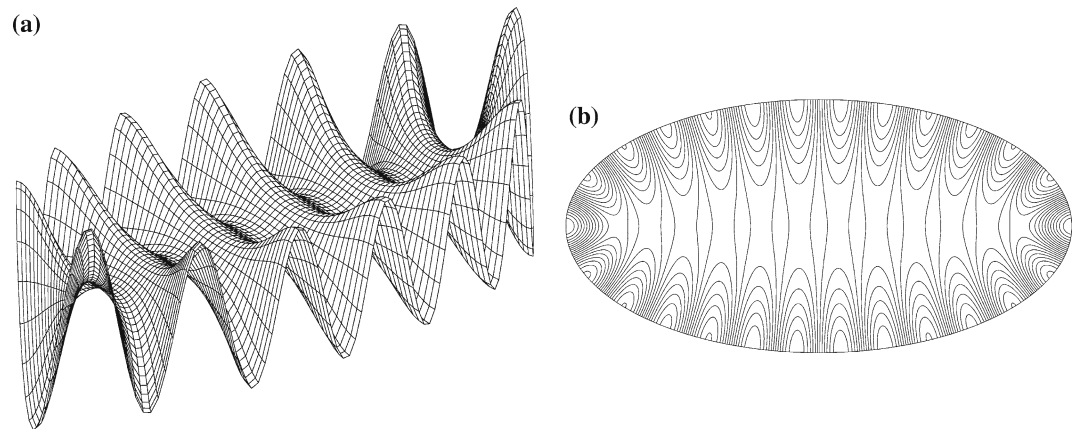

Fig. 5 Even hard mode 29 or $H^e_{13,1}$, $b/a = 1/2$, $ka = 19.13242517$. (**a**) Perspective view of ψ, (**b**) Contours of constant ψ

the $H^e_{13,1}$ mode of Fig. 5 is a "whispering gallery" type. Rather than employ the list of formulas available for different orders and q-values, a fast tri-diagonal eigenvalue solver obtains all characteristic values and series coefficients. Our functions do not provide convergence checks, but the number of series terms is included as an input parameter. A 50-term default value gives results agreeing well with tables in [3, 4], and [29]. However, available tables do not cover the large range of q-values desired in the current study. Because the parameter $q = \frac{1}{4}(ka)^2[1 - (b/a)^2]$ varies as the square of the frequency, the value of q can sometimes become large. Consider a high eccentricity case with $b/a = 0.1$. To compute the lowest 100 frequencies of the membrane, q-values approaching 2,000 are needed. Since the characteristic values and series coefficients for the Mathieu functions depend on an eigenvalue problem of infinite order, the finite-system order necessarily neglects the series coefficients beyond some chosen index order. A relatively small value, such as $q = 10$, gives a nearly diagonal matrix of eigenvectors. For instance, in evaluating the series (10) for $\mathrm{ce}_n(\eta, q)$ with small q, the coefficients A^n_m are small, except when m is close to n. A 50 term series is usually adequate for small q, but the series convergence becomes slower with increasing q. Consider Fig. 6 which uses a 100-term series to graph $\mathrm{Mc}^{(1)}_n(\xi_0, q)$ versus frequency ka and the function order n. The surface representation degenerates near the upper range of q and function order. Taking 150 terms is enough to remove this problem and allows accurate computation of frequencies for $0 < n < 80$ and $0 < ka < 500$. It turns out that the frequency parameter varies almost linearly with n and the root number p, giving a functional form $ka = c_0 + c_1 n + c_2 p$ where c_1 is considerably smaller than c_2. This means that, in computing, for example, the lowest 100 frequencies, one encounters higher function orders than might at first be expected. Even in the limiting case of a circular membrane with $b/a = 1$, the frequency of order 100 is $ka = 28.64019$ which is the first zero of $J_{23}(ka)$. Similarly, the elliptic membrane symmetric mode of order 100 for $b/a = 0.5$ gives $q = 303.1603$ as the first root of $\mathrm{Mc}^{(1)}_{19}(\xi_0, q)$.

Another noteworthy observation is that a pair of simple asymptotic formulae [9]

$$ka = \pi(p - 1/2)\frac{a}{b} + n + 1/2 + \frac{n^2 + n + 1}{\pi(4p - 2)}\frac{b}{a} \quad [p\text{th zero of } \mathrm{Mc}^{(1)}_n(\xi, q)], \tag{30}$$

$$ka = \pi p\frac{a}{b} + n + 1/2 + \frac{n^2 - n + 1}{4\pi p}\frac{b}{a} \qquad [p\text{th zero of } \mathrm{Ms}^{(1)}_n(\xi, q)], \tag{31}$$

are inapplicable unless p is large compared with the order n. This assertion is illustrated in Fig. 7 which shows two superimposed root surfaces pertaining to the case where $b/a = 0.5$. The lower surface, which is almost planar, gives the actual roots. The top surface graphs the asymptotic formula values which are obviously unsatisfactory for $p = 1$ and $n > 9$.

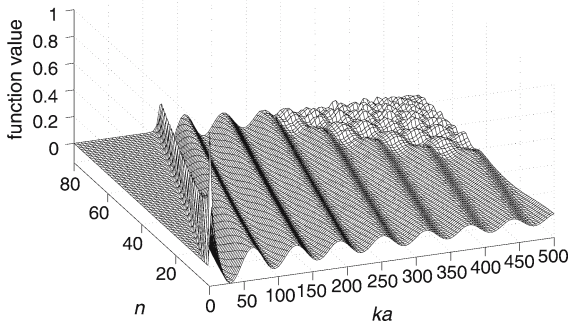

Fig. 6 Variation of $\mathrm{Mc}_n^{(1)}(\xi_0, q)$ with ka and n, Case: $b/a = 0.1$, $\xi_0 = \tanh^{-1}(b/a)$, $q = \frac{1}{4}(ka)^2[1 - (b/a)^2]$, 100 term series

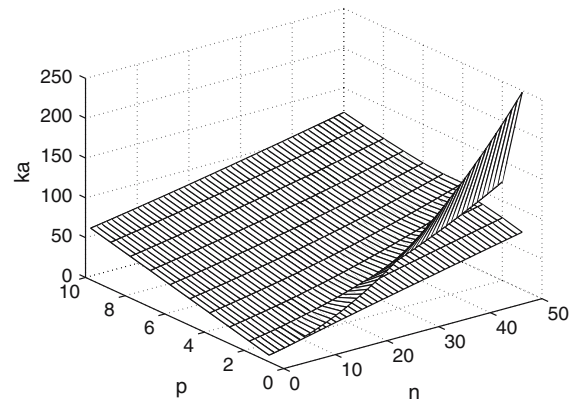

Fig. 7 pth root (ka) of $\mathrm{Mc}_n^{(1)}(\xi_0, q)$. Case: $b/a = 0.5$, $\xi_0 = \tanh^{-1}(b/a)$, $q = \frac{1}{4}(ka)^2[1 - (b/a)^2]$. Top surface: asymptotic approximation, Bottom surface: actual roots

Figure 8 illustrates how the series convergence relates to function order when q equals 10,000. The blank zone is the region outside of which all series coefficients are smaller than a chosen tolerance. For a typical function order, say 200, let M_{200} denote the largest magnitude of any series coefficient for this order. All coefficients that satisfy $|A_m^{200}| > \text{tol} * M_{200}$ lie within the range $40 < m < 150$. Figure 9 extends this idea to show, for several function orders and a range of q-values, the number of series terms adequate to assure that all neglected series coefficients fall below the specified tolerance.

5 Numerical evaluation using the Galerkin method

This section extends the method in [23] to include Neumann boundary conditions and assesses the accuracy of the Galerkin formulation in comparison to the "exact" solution in terms of Mathieu functions. A program computes the natural frequencies and presents graphical output identical with the analogous pro-

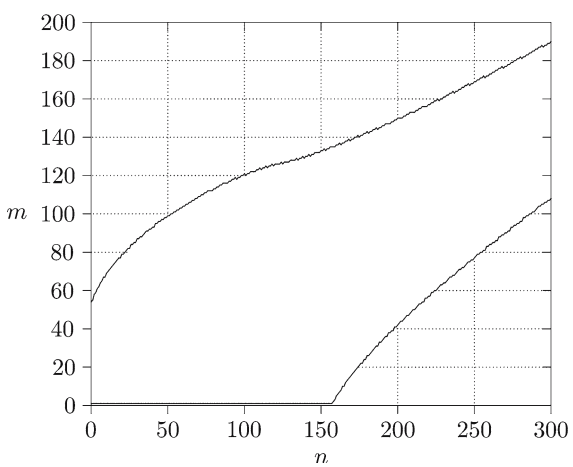

Fig. 8 Index range of dominant series coefficients in $\mathrm{ce}_n(z, q)$. Case: $q = 10^4$; tolerance $= 10^{-12}$

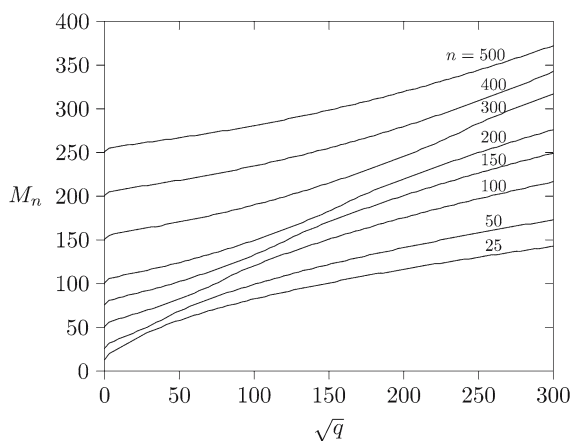

Fig. 9 Truncation index M_n of Fourier series such that $|A_m| < 10^{-12} \max |A_m|$ for $m > M_n$. Function order $n =$ 25, 50, 100, 150, 200, 300, 400, and 500

gram using Mathieu functions. The Galerkin program handles modes symmetric or anti-symmetric about the x-axis and Dirichlet or Neumann boundary conditions. No provision is made to treat separately modes symmetric or anti-symmetric about the y-axis in the manner characterized by even- or odd-order Mathieu functions. Besides the ellipse semi-diameters and a type parameter concerning symmetry and boundary conditions, the program input requires two values giving the number of circumferential and radial values defining a grid of collocation points covering the upper half of the ellipse. Also required are L and M of (23), two values specifying the number of approximating functions used for the radial and circumferential directions, respectively.

The numerical results in Tables 1–4, for $b/a = 1/2$, are obtained using 300 collocation points for each coordinate direction and 45 functions for each coordinate direction. Some finite-element results are also obtained using approximately 20,000 cubic elements and 70,000 nodes in the commercially available program FlexPde [30]. These approximate roots are rearranged according to the n and p indices which arrange Mathieu function-based frequencies in ascending order. The results in Tables 1 and 2 show agreement between the first 100 Galerkin and Mathieu function frequencies to at least six digits. It is clear that the finite-element software now available from commercial vendors handles high-frequency problems very well. The last column in Tables 1 and 2 also shows the asymptotic values of (30) or (31). Clearly, the asymptotic formulae are of limited quantitative value.

The results in Tables 3 and 4 pertain to a membrane with the Neumann (hard) boundary condition. The Mathieu and Galerkin results match less than those of the previous two tables but still agree to about five digits through the first 100 frequencies, as do the finite-element results.

Table 1 Resonant frequencies ka for soft, even modes E^e_{np}

I	n	p	Mathieu	Galerkin	Fin. elem.	Asymp.
1	0	1	3.77715586	3.77715587	3.77715235	3.72
2	1	1	5.01016192	5.01016193	5.01015335	4.88
3	2	1	6.33353033	6.33353035	6.33351458	6.20
4	3	1	7.71422171	7.71422173	7.71419742	7.68
5	4	1	9.13167372	9.13167375	9.13164021	9.31
6	0	2	9.97712016	9.97712012	9.97711522	9.95
7	5	1	10.57302174	10.57302179	10.57297886	11.11
8	1	2	11.07869692	11.07869687	11.07869009	11.00
9	6	1	12.02991059	12.02991065	12.02985839	13.06
10	2	2	12.22517262	12.22517257	12.22516339	12.11
11	3	2	13.41144729	13.41144722	13.41143497	13.27
12	7	1	13.49662286	13.49662293	13.49656171	15.18
13	4	2	14.63293864	14.63293856	14.63292264	14.48
14	8	1	14.96900296	14.96900304	14.96893366	17.45
15	5	2	15.88565752	15.88565742	15.88563707	15.75
16	0	3	16.24823969	16.24823979	16.24823443	16.22
17	9	1	16.44383320	16.44383329	16.44375669	19.88
18	6	2	17.16623204	17.16623192	17.16620613	17.07
19	1	3	17.32773381	17.32773392	17.32772683	17.26
20	10	1	17.91847260	17.91847270	17.91838997	22.47
30	13	1	22.32015058	22.32015070	22.32006015	31.20
40	12	2	25.31322551	25.31322523	25.31316397	26.09
50	14	2	28.17189035	28.17188999	28.17182255	29.52
60	2	5	30.95381867	30.95381904	30.95384889	30.84
70	21	1	33.73392302	33.73392026	33.73387615	61.49
80	16	3	36.08259485	36.08259546	36.08266412	36.55
90	24	1	37.91528358	37.91534021	37.91525933	75.47
100	19	3	40.21013472	40.21014918	40.21232734	41.27

Case: $b/a = 1/2$; pth value of ka such that $\mathrm{Mc}_n^{(1)}(\xi_0, q) = 0$. where $q = \frac{1}{4}(ka)^2[1 - (b/a)^2]$ and $\xi_0 = \tanh^{-1}(b/a)$

Table 2 Resonant frequencies ka for soft, odd modes E^o_{np}

I	n	p	Mathieu	Galerkin	Fin. elem.	Asymp.
1	1	1	6.85176340	6.85176340	6.85175953	6.82
2	2	1	7.98096836	7.98096836	7.98096204	7.90
3	3	1	9.17017540	9.17017540	9.17016551	9.06
4	4	1	10.40781192	10.40781192	10.40779727	10.30
5	5	1	11.68407134	11.68407134	11.68405092	11.62
6	6	1	12.99089339	12.99089339	12.99086645	13.02
7	1	2	13.11107543	13.11107543	13.11106945	13.09
8	2	2	14.19879782	14.19879782	14.19879030	14.13
9	7	1	14.32175778	14.32175778	14.32172367	14.49
10	3	2	15.32171724	15.32171724	15.32170800	15.21
11	8	1	15.67142165	15.67142165	15.67138019	16.05
12	4	2	16.47686461	16.47686461	16.47685319	16.33
13	9	1	17.03566767	17.03566767	17.03561907	17.69
14	5	2	17.66143700	17.66143700	17.66142319	17.48
15	10	1	18.41108976	18.41108976	18.41103414	19.40
16	6	2	18.87282777	18.87282777	18.87281121	18.68
17	1	3	19.38694084	19.38694084	19.38693588	19.36
18	11	1	19.79492161	19.79492161	19.79486001	21.20
19	7	2	20.10864040	20.10864040	20.10862096	19.92
20	2	3	20.46098453	20.46098453	20.46097832	20.39
30	6	3	24.98869886	24.98869886	24.98869450	24.76
40	13	2	27.92706712	27.92706712	27.92703053	28.19
50	11	3	31.07713445	31.07713446	31.07714137	30.82
60	13	3	33.61883169	33.61883170	33.61884501	33.43
70	15	3	36.21103129	36.21103129	36.21108739	36.15
80	7	5	38.54496121	38.54496122	38.54505481	38.26
90	26	1	40.68935279	40.68943445	40.68959892	57.69
100	20	3	42.87782317	42.87783005	42.88392356	43.40

Case: $b/a = 1/2$; pth value of ka such that $\mathrm{Ms}_n^{(1)}(\xi_0, q) = 0$. where $q = \frac{1}{4}(ka)^2[1 - (b/a)^2]$ and $\xi_0 = \tanh^{-1}(b/a)$

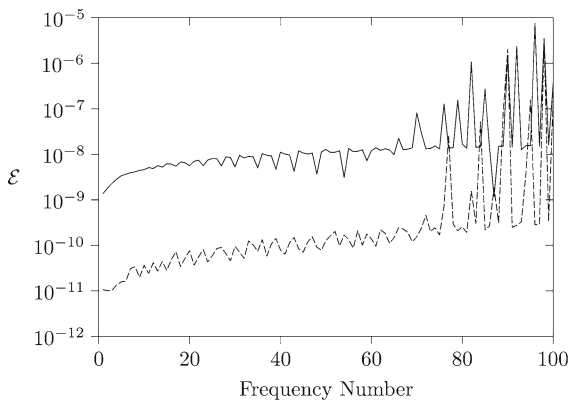

Fig. 10 Relative error between Galerkin and Mathieu methods to compute resonant frequencies. Case: $b/a = 1/2$. Solid curve: even modes, dashed curve: odd modes. Modified Mathieu functions series terminated at 200 terms. Galerkin method with 45 radial and 45 circumferencial functions

Figure 10 shows how the Mathieu $(ka)_M$ and Galerkin $(ka)_G$ natural frequencies compare for the Dirichlet boundary condition. The relative error measure is

$$\mathcal{E} = \left| \frac{(ka)_G - (ka)_M}{(ka)_M} \right|. \tag{32}$$

The accuracy of the Galerkin method for this case where $b/a = 1/2$ is quite good. Comparable accuracy holds for larger b/a values. However, accuracy decreases as b/a becomes small. For example, when

Table 3 Resonant frequencies ka for hard, even modes H^e_{np}

I	n	p	Mathieu	Galerkin	Fin. elem.
1	1	1	1.87357563	1.87356286	1.87356721
2	2	1	3.41903131	3.41900589	3.41901344
3	3	1	4.92906598	4.92902673	4.92903872
4	4	1	6.41801765	6.41796305	6.41798179
5	0	1	6.76024730	6.76021414	6.76024378
6	1	2	7.87147773	7.87143470	7.87147216
7	5	1	7.88925340	7.88918154	7.88921013
8	2	2	9.04814696	9.04809344	9.04813814
9	6	1	9.34361693	9.34352552	9.34356756
10	3	2	10.28174582	10.28168170	10.28173215
11	7	1	10.78147167	10.78135823	10.78141749
12	4	2	11.56493082	11.56485647	11.56491055
13	8	1	12.20349662	12.20335862	12.20343874
14	5	2	12.89119042	12.89110652	12.89116189
15	0	2	13.06856493	13.06850475	13.06855971
16	9	1	13.61095438	13.61078947	13.61089369
17	1	3	14.15137926	14.15130998	14.15137251
18	6	2	14.25447208	14.25437942	14.25443419
19	10	1	15.00561142	15.00541750	15.00554881
20	2	3	15.26955646	15.26947758	15.26954819
30	0	3	19.35924738	19.35915684	19.35924815
40	3	4	22.64703345	22.64691428	22.64703252
50	14	2	25.87945557	25.87929585	25.87937144
60	8	4	28.54914442	28.54897195	28.54916673
70	10	4	31.03110041	31.03090554	31.03114303
80	19	2	33.29248637	33.29226329	33.29253430
90	3	6	35.16371615	35.16353883	35.16382360
100	15	4	37.47393937	37.47368819	37.47474816

Case: $b/a = 1/2$; pth value of ka such that $\mathrm{Mc}_n^{(1)\prime}(\xi_0, q) = 0$. where $q = \frac{1}{4}(ka)^2[1 - (b/a)^2]$ and $\xi_0 = \tanh^{-1}(b/a)$

$b/a = 0.2$, the error measure is about 10^{-9}, 10^{-2}, and 10^{-1} for frequency numbers 20, 50, and 100, respectively.

Such quantitative results provide confidence in the validity of the Galerkin method in this problem and in the correctness of the computed Mathieu functions. A primary reference which motivated our interest in the elliptic membrane problem is the paper by Chen et al. [6], which deals primarily with relatively high-frequency modes of a nearly circular membrane having $a = \cosh 2$ and $b = \sinh 2$ so that $b/a = 0.9640$. Table 1 of [6] presents frequencies derived from the first seven roots of the modified Mathieu functions $\mathrm{Ce}_n(z, q) = \mathrm{Mc}_n^{(1)}(z, q)$ for $n = 0, 1, \ldots, 6$ and $\mathrm{Se}_n(z, q) = \mathrm{Ms}_n^{(1)}(z, q)$ for $n = 1, 2, \ldots, 6$ for their specially chosen semi-diameter ratio. Our comparable Mathieu function roots shown in Table 5a agree with some but not all of the values in Table 5b from [6]. The numerical data in Table 5a is valid, as evidenced by the five-digit agreement between the Mathieu function evaluations and the independent Galerkin calculations.

6 Conclusions

This study was conducted to produce some readily available MATLAB routines for angular and radial Mathieu functions, useful in various physical problems where elliptic coordinates are involved. These routines have been successfully applied to elliptic membrane modal analysis for high frequencies. Continuing interest in this canonical eigenvalue problem, by researchers in electromagnetics and wave physics, is indicated

Table 4 Resonant frequencies ka for hard, odd modes H^o_{np}

I	n	p	Mathieu	Galerkin	Fin. elem.
1	1	1	3.53539992	3.53538074	3.53539856
2	2	1	4.64124553	4.64121380	4.64124293
3	3	1	5.83516485	5.83511792	5.83515924
4	4	1	7.08895334	7.08888914	7.08894270
5	5	1	8.38235005	8.38226684	8.38233280
6	6	1	9.70150067	9.70139685	9.70147590
7	1	2	9.91905186	9.91900559	9.91904705
8	2	2	11.01193392	11.01187835	11.01192740
9	7	1	11.03709039	11.03696440	11.03705790
10	3	2	12.15024012	12.15017462	12.15023144
11	8	1	12.38285996	12.38271021	12.38281999
12	4	2	13.32909409	13.32901822	13.32908260
13	9	1	13.73458698	13.73441185	13.73453989
14	5	2	14.54396048	14.54387392	14.54394551
15	10	1	15.08942048	15.08921835	15.08936679
16	6	2	15.79067193	15.79057450	15.79065287
17	1	3	16.21470352	16.21462923	16.21469839
18	11	1	16.44544806	16.44521728	16.44538844
19	7	2	17.06542284	17.06531446	17.06539961
20	2	3	17.29105294	17.29096964	17.29104650
30	15	1	21.86231030	21.86194904	21.86223829
40	3	4	24.66128486	24.66116414	24.66128738
50	6	4	28.04849016	28.04834006	28.04850549
60	13	3	30.67030677	30.67010788	30.67031977
70	5	5	33.14329074	33.14312252	33.14334609
80	25	1	35.29333207	35.29254819	35.29366785
90	9	5	37.73806113	37.73785249	37.73824506
100	5	6	39.39968721	39.39949013	39.40066116

Case: $b/a = 1/2$; pth value of ka such that $\mathrm{Ms}_n^{(1)\prime}(\xi_0, q) = 0$. where $q = \frac{1}{4}(ka)^2[1 - (b/a)^2]$ and $\xi_0 = \tanh^{-1}(b/a)$

by recently published papers and numerous downloads of our programs from the MathWorks archive. Galerkin results compare well with the numerical evaluations from the Mathieu functions. The conceptually elementary Galerkin procedure also yields resonant frequencies that compare well with finite-element programs utilizing cubic elements.

Many recent publications include graphs and numerical results that were heretofore difficult, at best, to obtain by researchers primarily interested in applying the Mathieu functions to physical problems. The present work has centered around the eigenmodes of the Helmholtz equation in the context of waves in the interior of an elliptic cylinder, but the calculations for the modified Mathieu functions of the first kind are readily modified to handle the functions of the second kind, where the appropriate linear combination satisfies the radiation condition required in exterior problems. Accurate numerical computation of the high frequencies is much harder than for low frequencies. The key step in computing both the angular (periodic) and the radial (modified) Mathieu functions is the solution of the eigenvalue problem for the underlying tridiagonal matrix that results from requiring periodicity in the angular functions. The two-parameter dependence of the Mathieu functions, the nonexistence of any explicit formulae for their evaluation, and the implicit occurrence of the order all contribute to the complications inherent in the calculation of these eigenfunctions of the Helmholtz equation that arise by separating variables in elliptic coordinates. Continuing and future work includes the extension to handle complex values of the frequency parameter q resulting from a physically lossy medium. As in the above work with real q, the high frequency (large $|q|$) calculations present numerical difficulties, and a direct asymptotic analysis of Mathieu's differential equation offers some guidance and validation.

Table 5 Values for comparison with Table 1 of Chen et al. [6]

(a) Roots from the present Mathieu functions							
Ce_0	0.65123129	1.49784709	2.35503473	3.21749355	4.08203631	4.94732666	5.81293426
Ce_1	1.02808007	1.88387435	2.73593614	3.59120969	4.45108137	5.31394325	6.17818689
Se_1	1.04707973	1.91835590	2.78411713	3.64924648	4.51454935	5.38008827	6.24580297
Ce_2	1.38747716	2.26882690	3.12671219	3.97901777	4.83233042	5.68947135	6.55017420
Se_2	1.39069100	2.28073785	3.15122897	4.01676291	4.88119341	5.74569041	6.61051077
Ce_3	1.72602682	2.63820326	3.51256008	4.37137203	5.22392323	6.07591028	6.93070787
Se_3	1.72633659	2.64047266	3.52057045	4.38936664	5.25397302	6.11736398	6.98077514
Ce_4	2.05326710	2.99268176	3.88482152	4.75670224	5.61649374	6.46963032	7.32089967
Se_4	2.05328995	2.99296217	3.88639120	4.76219234	5.62975373	6.49354625	7.35599793
Ce_5	2.37354289	3.33789876	4.24575752	5.13015765	6.00083943	6.86162875	7.71565472
Se_5	2.37354435	3.33792596	4.24597533	5.13123875	6.00462084	6.87133730	7.73452314
Ce_6	2.68877579	3.67658787	4.59920934	5.49462815	6.37490193	7.24488262	8.10659696
Se_6	2.68877588	3.67659013	4.59923384	5.49478863	6.37564532	7.24748867	8.11363424
(b) Roots from Table 1 of Chen et al. [6]							
Ce_0	0.65123129	1.49784709	2.35503473	3.21749843	4.08203626	4.94732655	5.81293420
Se_0			2.28073760	3.15122897	4.01676288	4.88119330	5.74569056
Ce_1	1.02808007	1.88388127	2.73593640	3.59120982	4.45108722	5.31394317	6.17818679
Se_1		1.91833607	2.78409872	3.64927690	4.51451132	5.38008810	6.24580307
Ce_2	1.38747716	2.26882701	3.12071201	3.97901797	4.83233029	5.68947133	6.55017404
Se_2		2.25732054	3.11618100	3.96794909	4.81647132	5.66328950	6.50920610
Ce_3	1.72602682	2.63820326	3.51256008	4.37137203	5.22392323	6.07591028	6.93070787
Se_3		2.64047268	3.52057041	4.38936670	5.25397297	6.11736414	6.98077503
Ce_4	2.05326667	2.99268174	3.88482175	4.75670222	5.61649357	6.46963028	7.32089967
Se_4	2.27770674	3.14260402	3.99863927	4.84906259	5.69457215	6.53473244	7.36814414
Ce_5	2.37354250	3.33789874	4.24766336	5.13015750	6.00083927	6.86162867	7.71565474
Se_5	2.37354419	3.38792570	4.24597551	5.13123884	6.00462089	6.87133728	7.73452313
Ce_6	2.68877593	3.67658809	4.59920950	5.49462839	6.37490204	7.24488261	8.10659707
Se_6	3.14538710	4.00495543	4.86085219	5.71422751	6.56520281	7.41315641	8.25650774

Case: $a = \cosh 2$ and $b = \sinh 2$ such that $\xi_0 = 2$ First 7 roots (ka) of $\mathrm{Ce}_n(\xi_0, q)$ and $\mathrm{Se}_n(\xi_0, q)$, with $q = \frac{1}{4}(ka)^2[1 - (b/a)^2]$

Acknowledgements The authors wish to thank Professor W.H. Butler of the Center for Materials for Information Technology (MINT) at the University of Alabama, for providing access to shared facilities provided by the NSF-MRSEC grant DMR0213985.

References

1. McLachlan NW (1947) Theory and application of Mathieu functions. Oxford University Press, London
2. Meixner J, Schäfke FW (1954) Mathieusche Funktionen und Sphäroidfunktionen. Springer-Verlag, Berlin
3. Abramowitz M, Stegun IA (1972) Handbook of mathematical functions with formulas, graphs, and mathematical tables. National Bureau of Standards, Washington, DC
4. Zhang S, Jin J (1996) Computation of special functions. Wiley, New York
5. Gutiérrez-Vega JC, Rodríguez-Dagnino RM, Meneses-Nava MA, Chávez-Cerda S (2003) Mathieu functions, a visual approach. Am J Phys 71:233–242
6. Chen G, Morris PJ, Zhou J (1994) Visualization of special eigenmode shapes of a vibrating elliptical membrane. SIAM Rev 36:453–469
7. Keller JB, Rubinow SI (1960) Asymptotic solution of eigenvalue problems. Ann Phys 9:24–75
8. Akulenko LD, Nesterov SV (2000) Free vibrations of a homogeneous elliptic membrane. Mech Solids 35:153–162
9. Troesch BA, Troesch HR (1973) Eigenfrequencies of an elliptic membrane. Math Comp 27:755–765
10. Ancey S, Folacci A, Gabrielli P (2001) Whispering-gallery modes and resonances of an elliptic cavity. J Phys A: Math Gen 34:1341–1359
11. Alhargan FA (1996) A complete method for the computations of Mathieu characteristic numbers of integer orders. SIAM Rev 38:239–255
12. Alhargan FA (2000) Algorithms for the computation of all Mathieu functions of integer orders. ACM Trans Math Software 26:390–407

13. Alhargan FA (2000) Algorithm 804: Subroutines for the computation of Mathieu functions of integer orders. ACM Trans Math Software 26:408–414
14. Hunter G, Kuriyan M (1976) Asymptotic expansions of Mathieu functions in wave mechanics. J Comput Phys 21:319–325
15. Canosa J (1971) Numerical Solution of Mathieu's Equation. J Comput Phys 7:255–272
16. Frenkel D, Portugal R (2001) Algebraic methods to compute Mathieu functions J Phys A: Math Gen 34:3541–3551
17. Stamnes JJ, Spjelkavik B (1995) New method for computing eigenfunctions (Mathieu functions) for scattering by elliptical cylinders. Pure Appl Opt 4:251–262
18. Zhang S, Shen Y (1995) Eigenmode sequence for an Elliptical waveguide with arbitrary ellipticity. IEEE Trans. Microwave Theory Tech 43:227–230
19. Schneider M, Marquardt J (1999) Fast computation of modified Mathieu functions applied to elliptical waveguide problems. IEEE Trans Microwave Theory Tech 47:513–516
20. Moler CB (2004) Numerical computing with MATLAB. SIAM, Philadelphia
21. Aunola M (2003) The discretized harmonic oscillator: Mathieu functions and a new class of generalized Hermite polynomials. J Math Phys 44:1913–1936
22. Arfken GB, Weber HJ (2005) Mathematical methods for physicists, 6th edn. Elsevier Academic Press, London
23. Wilson HB, Turcotte LS, Halpern D (2003) Advanced mathematics and mechanics applications using MATLAB, 3rd edn. Chapman & Hall/CRC, Boca Raton
24. Kantorovich LV, Krylov VI (1958) Approximate methods of higher analysis. P. Noordhoff Ltd, Groningen
25. Fox L, Henrici P, Moler C (1967) Approximations and bounds for eigenvalues of elliptic operators. SIAM J Numer Anal 4:89–102
26. Driscoll TA (1997) Eigenmodes of isospectral drums. SIAM Rev 39:1–17
27. Platte RB, Driscoll TA (2004) Computing eigenmodes of elliptic operators using radial basis functions. Comput Math Applics 48:561–576
28. Wilson HB (2004) Vibration modes of an elliptic membrane. http//www.mathworks.com/matlabcentral/fileexchange MATLAB File Exchange, The MathWorks, Natick, MA
29. Blanch G, Clemm DS (1962) Tables relating to the radial Mathieu functions, vol. 1 Functions of the first kind. Aeronautical Research Laboratories, US Air Force, Washington, DC
30. Backstrom G (2005) Simple fields of physics by finite element analysis. GB Publishing, Uppsala